Proceedings of the Pressure Vessels and Piping Conference
SAND2017-1454C
PVP2017
July 16-20, 2017, Hilton Waikoloa Village, Hawaii, USA

PVP2017-65992

THERMAL MECHANICAL FINITE ELEMENT SIMULATION OF ADDITIVE MANUFACTURING; PROCESS MODELING OF THE LENS PROCESS

Michael E. Stender
Sandia National Laboratories
Livermore, CA, USA

Lauren L. Beghini
Sandia National Laboratories
Livermore, CA, USA

Michael G. Veilleux
Sandia National Laboratories
Livermore, CA, USA

Samuel R. Subia
Sandia National Laboratories
Livermore, CA, USA

Joshua D. Sugar
Sandia National Laboratories
Livermore, CA, USA

ABSTRACT

Laser engineered net shaping (LENS) is an additive manufacturing process that presents a promising method of creating or repairing metal parts not previously feasible with traditional manufacturing methods. The LENS process involves the directed deposition of metal *via* a laser power source and a spray of metal powder co-located to create and feed a molten pool (also referred to generically as Directed Energy Deposition, DED). DED technologies are being developed for use in prototyping, repair, and manufacturing across a wide variety of materials including stainless steel, titanium, tungsten carbide-cobalt, aluminum, and nickel based superalloys. However, barriers to the successful production and qualification of LENS produced or repaired parts remain. This work proposes a finite element (FE) analysis methodology capable of simulating the LENS process at the continuum length scale (*i.e.* part length scale). This method proposes an element activation scheme wherein only elements that exceed the material melt temperature during laser heating are activated and carried through to subsequent analysis steps. Following the initial element activation calculation, newly deposited, or activated elements and the associated geometry, are carried through to thermal and mechanical analyses to calculate heat flow due to radiation, convection, and conduction as well as stresses and displacements. The final aim of this work is to develop a validated LENS process simulation capability that can accurately predict temperature history, final part shape, distribution of strength, microstructural properties, and residual stresses based on LENS process parameters.

INTRODUCTION

Recent advances in additive manufacturing (AM) have enabled previously impossible to manufacture parts to be built and designed using directed energy deposition methods (DED) (1,2). A common way to build metal parts using AM is the controlled melting of metal powders. Three primary powder based metal AM methods have emerged including laser engineered net shaping (LENS) (3), powder-based electron beam powder bed manufacturing (EBPB) (4), and laser based powder-bed manufacturing (1). This work focuses on analysis methodologies developed to model the LENS process. The LENS method uses a spray of metal powder co-located with a laser heat source to create and feed a molten pool of metal, progressively building up a geometry following solidification (4). Because of the layered nature of LENS manufacturing, complex geometries can be easily created. In addition to the manufacturing of previously difficult or impossible to manufacture part geometries (5), LENS has been used in a range of industrial prototyping and repair applications (6). A wide range of metal materials have been used in the LENS process including steel (7, 8), titanium (9) tungsten carbide-cobalt (10), nickel-based super alloys (11), intermetallic Fe-Al alloys (12), and aluminum (13). The ability of the LENS process to manufacture, repair, and prototype complex geometries in a wide range of materials, and/or material combinations makes LENS an attractive option for continued use (14). However, uncertainties in thermal conditions during processing, as well as post-processing residual stresses and microstructure must be better understood and quantified prior to full confidence LENS production of critical components.

Thermal conditions during the LENS process involve peak temperatures at or above melt temperature, and cyclical

heating as successive heating passes reheat and/or remelt material (14). Characterization of thermal conditions during the LENS process is of great importance because thermal conditions are understood to have a significant influence on the geometry, residual stress state, and microstructure in the resulting part (14). Cooling rate during traditional forging is understood to affect the microstructure, and consequently, mechanical properties in steel (15). Compared with forging, LENS builds experience much higher cooling rates (16). Models developed to simulate the dendritic solidification structure during cooling in LENS material demonstrate the influence of cooling rate on LENS microstructure (16). Additionally, cooling rates in traditional forgings are known to have an influence on the decomposition from austenite to ferrite in steel (17). Similar phase effects are likely present in LENS process and are likely influenced by the specific thermal history (14). Process parameters specific to the LENS process such as laser power, substrate size, and substrate preheat have been shown to be influential on the LENS thermal environment (14). Thermal finite element models have been applied to simulate the temperature field during the LENS process in 2D (18) and 3D (19) as well as to optimize laser power to maintain a constant sized melt pool (20). Additionally, substrate preheat has been shown to be a way to reduce some residual stress in LENS builds (21). Despite some similarities with traditional forging, LENS manufacturing exhibits some critical differences in thermal histories and microstructure that must be better understood prior to full confidence production.

Finite element (FE) modeling has emerged as a method of simulating the LENS process and powder bed AM and may help increase confidence and understanding in LENS part properties (18, 19, 20, 22, 23 24). One challenge associated with the implementation of a FE model of the LENS process is the need to account for the addition of material as a build progresses (18). Wang *et al*. (20) implemented a block-by-block element activation strategy wherein each complete layer of elements for a pass was activated and then heated *via* a moving laser heat source. Accurate and precise thermal modeling is essential because temperature distributions are strong indicators of residual stress magnitudes (25) and microstructure in steel (16). Residual stresses in LENS builds are of concern due to the potential of causing part distortion and/or premature failure. Residual stress measurements in powder bed manufacturing, a similar DED process to LENS, showed relatively high magnitudes of residual stress (~100-500 MPa) in 316L stainless steel (23). Because of the coupled nature of the temperature profiles and residual stresses, full thermal-mechanical coupling would enable the most accurate FE solution for the LENS process. Hodge *et al*. (22) implemented a coupled thermal-mechanical finite element methodology for modeling the powder bed manufacturing process. An accurate predictive capability for the LENS process that captures the effects of process parameters such as substrate preheat, laser scan pattern, laser power, and substrate size could be used to help mitigate the negative effects of residual stresses and other factors inherent to the LENS process.

A long history of empirical, experimental and modeling data is available for traditionally manufactured parts (27, 28, 29). However, there is no such knowledge base to draw from for LENS manufacturing. The challenge with producing high-confidence LENS parts lies in developing an understanding analogous to the knowledge base available for traditional manufacturing methods in an accelerated timeframe. The overreaching aim of this work is to develop and implement an appropriate FE methodology for the continuum-scale simulation off the LENS process. Such a tool could be used with appropriate experimental data to develop an improved understanding of the LENS process without requiring extensive experimental testing (30). The modeling challenges associated with the LENS process addressed in this work include: 1) activation, or 'birthing' of elements associated with material deposition, 2) tracking and/or initializing the evolving thermal and mechanical states in newly activated and previously active elements, and 3) representing both solid and fluid phases during melting and solidification. This work proposes a finite element methodology using the SIERRA Multiphysics code suite developed at Sandia National Laboratories (31, 32). The proposed methodology incorporates, laser scan speed, laser raster pattern, laser power, laser efficiency, substrate dimensions, substrate preheat, and deposition and substrate materials. The proposed methodology may be useful in simulating the LENS process and helping to understand and mitigate the negative effects of residual stresses and/or thermal conditions to improve LENS part performance and functionality

NOMENCLATURE

AM – Additive Manufacturing
LENS – Laser Engineered Net Shaping
DED – Directed Energy Deposition
FE – Finite Element
CFD – Computational Fluid Dynamics
EBAM – Electron Beam Additive Manufacturing

METHODS

In this LENS simulation FE methodology, laser power is characterized as a spherical heat source moving through a volume of initially inactive elements. Two classifications of elements are defined as, 1) active elements that are initially present in the computational domain and 2) inactive elements which can be switched to active status based on the applied heating. Thus, the computational domain as used herein can be decomposed into two regions including a substrate block which contains all initially active elements such as a build plate and/or other nearby parts, and a deposition block which is composed of initially inactive elements that can be activated by a laser heat source when heated above material melt temperature. To model deposition in LENS, a thermally-based element activation scheme is carried out wherein only inactive elements that exceed the material melt temperature following laser heating are activated and carried through to subsequent analysis steps. Initially, elements in the deposition block are defined to have zero conductivity to ensure only regions that are heated to above

the material melt temperature are activated. Each time step in the overall analysis is calculated using a sequence of thermal analyses (first to determine which elements are activated, and then to calculate heat transfer), mapping operations, and a structural analysis. The sequence of solution steps that occurs within each time step is outlined as follows and is illustrated in Figure 1.

1) An initial thermal calculation is run to determine if and where elements are activated (*i.e.* if inactive elements are heated to above melt temperature). The laser heat source is passed through the deposition block and elements that reach a temperature above the defined material melt temperature are switched to active status and tracked.
2) A script creates a new mesh containing only active elements. Additionally, surfaces are defined on the outer regions of the activated part for radiation and convection calculations.
3) A traditional heat transfer thermal analysis is performed to calculate temperatures throughout the active mesh from the previous step by applying conduction, radiation, and convection through the appropriate surfaces.
4) An algorithm initializes newly activated elements with predetermined material parameters as specified for near melt material behavior. Also, because the thermal analysis steps do not track mechanical properties, previously calculated displacements and material state variables are also transferred to the current mesh.
5) A traditional structural analysis is performed to calculate residual stresses. Temperature distributions are included and used to calculate thermal expansion and to include temperature dependent material parameters.
6) Finally, all values including state variables, displacements, and temperatures are mapped back to the original mesh.

This sequential process outlined above is completed for each time step until the desired completion time is reached.

For all analyses both substrate and deposition blocks were modeled as 304L stainless steel. A temperature dependent elastic-plastic constitutive model for 304L stainless steel was used. Material parameters used were determined previously for forging processes (33, 34, 35). A Young's modulus of 200 GPa and a Poisson's ratio of 0.249 were used. The material melt temperature was defined as 1700 K. Solid and liquid phases were tracked based on element temperature relative to the material melt temperature. Elements with temperatures above the defined material melt temperature were treated as liquid and elements below material melt temperature were treated as solid. For liquid elements, a Newtonian fluid constitutive model was used and contact was modeled using a frictional-sliding contact algorithm. Below the material melt temperature, the elastic-plastic constitutive model, was used and contact was modeled using a tied contact algorithm. For liquid elements, a fluid viscosity of 1.0e-6 kg/(s*m) and a fluid bulk modulus of 2.2e9 Pa were used. A constant emissivity of 0.25 was used for all elements.

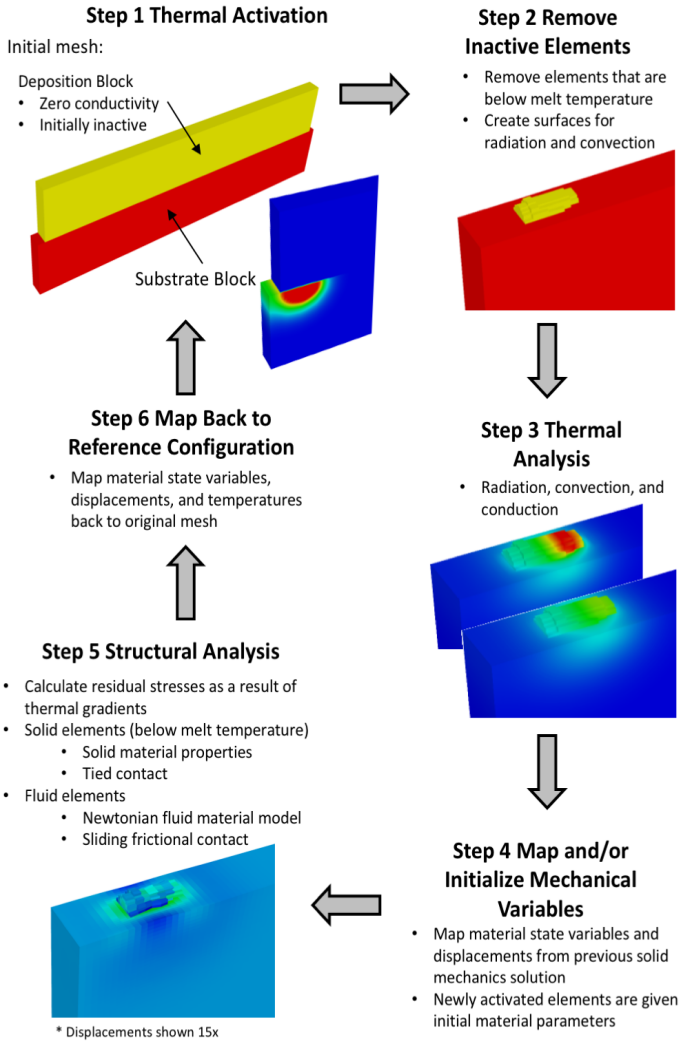

FIGURE 1. OUTLINE OF SOLUTION PROCESS FOR LENS MODELING. AS SHOWN, EACH COMPLETE CYCLE CORRESPONDS TO A SINGLE TIME STEP.

To demonstrate the proposed methodology, two FE models were created. The first, (Figure 2, top) is a cylindrical build on a large substrate. A constant 500 W laser with a 0.001 m beam diameter, a helical scan pattern, a scan rate of 20 in/min, and a 36% laser efficiency was used. Displacements on the bottom surface of the substrate were held fixed. The second FE model, (Figure 2, bottom) is a thin walled part (*i.e.* roughly a single laser beam width) on a thin substrate. For the thin walled build model, laser powers of both 500 W and 2000 W and beam diameters of 0.001 m and 0.0025 m, respectively were used. To avoid inverted elements, an additional variable laser power thin walled build model, where laser power was reduced steadily from 500 W to 250 W over the 2 build passes was developed. Laser efficiency

was defined to be 36%, and a laser scan speed of 20 in/min was used. For all models, the bottom surface of the substrate was defined to have a 293.15 K constant temperature (20 °C) and displacements on the bottom of the substrate were held fixed. A fixed time step of 0.05 seconds was used. For both FE models, hexahedral 3D elements were used. The thin walled model had 302,400 and 194,560 in the substrate block and the deposition block, respectively. The cylindrical button model had 4,800 and 54,875 elements in the substrate block and the deposition block, respectively. All simulations were run in parallel using 64 processors.

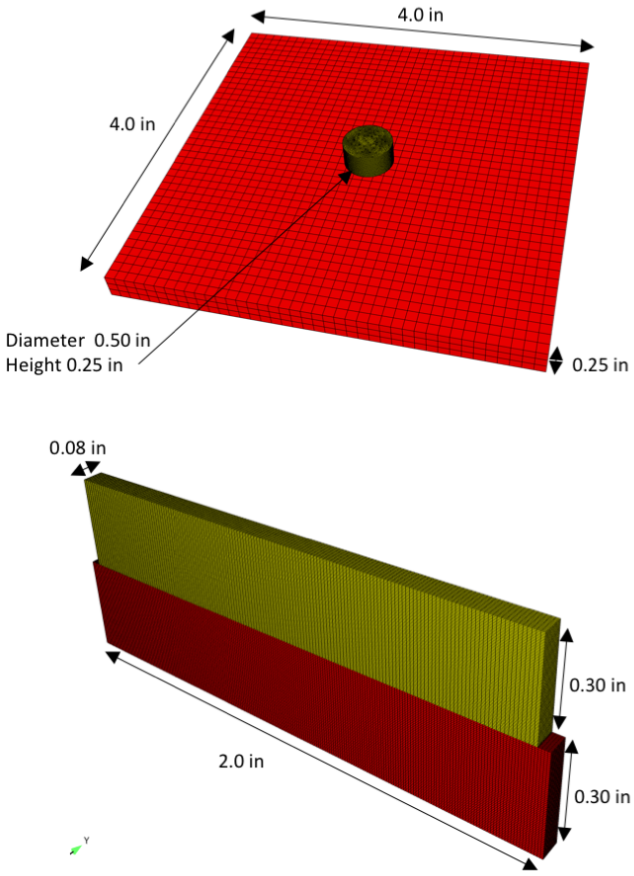

FIGURE 2. CYLINDER (TOP) AND THIN WALL (BOTTOM) FINITE ELEMENT MODELS FOR LENS SIMULATION. YELLOW CORRESPONDS TO THE DEPOSITION BLOCK AND RED CORRESPONDS TO THE SUBSTRATE.

RESULTS

FE solutions were calculated for thin walled and cylindrical builds using the 500 W laser model. Both 500 W and 2000 W laser model experienced inverted elements during the solid mechanics calculation step and thus, only thermal results are available. Solution calculation time was highly dependent on the number of elements used. With increasing numbers of active elements as a part is built, up the computational time required for each time step increases.

500 W and 2000 W laser power and 0.001 m and 0.0025 m beam diameters, respectively in the thin walled model showed differential thermal and element activation responses (Figure 3). For one 0.05 second time step, higher laser power and a larger beam diameter resulted more activated elements (*i.e.* more deposited material) and higher substrate and deposited part temperatures as shown in Figure 3.

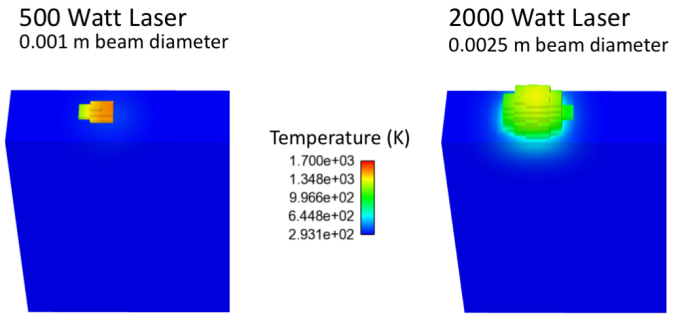

FIGURE 3. DIFFERENTIAL ACTIVATION AND TEMPERATURE RESPONSE WITH VARYING LASER POWER FOR 0.05 SECONDS OF LENS BUILD TIME.

Later in the build process, thermal differences between 2000 W and 500 W laser powers were also evident. The 2000 W laser model showed a larger melt pool, and significantly higher temperatures in both the deposited region and the substrate compared to the 500 W model (Figure 4.)

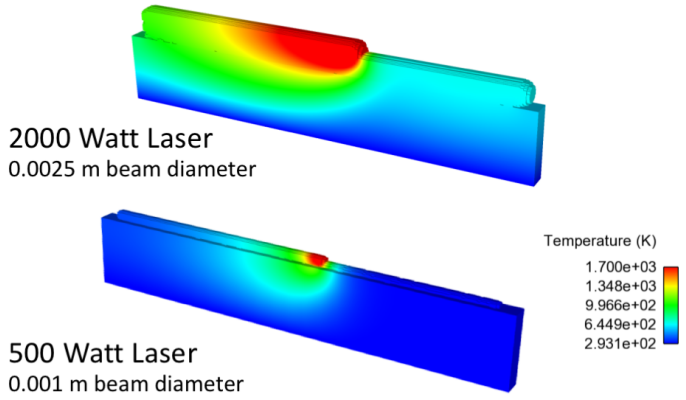

FIGURE 4. DIFFERENTIAL THERMAL RESPONSES OF THIN WALL MODEL AFTER 1.5 DEPOSITION PASSES WITH 2000 WATT AND 500 WATT LASER POWERS USING 0.001 M AND 0.0025 M LASER BEAM DIAMETERS, RESPECTIVELY.

For the variable laser power thin walled build model, stresses began to build during deposition, and slightly increased in magnitude following cooling to room temperature. Generally, the magnitudes of axial stress increased once reaching the final build state at room temperature as compared to during the build

(Figure 5). Axial stress magnitudes were lower near the beginning and end of each deposition pass as compared to the middle of the pass. Temperature profiles with the variable laser power thin walled model show a relatively constant and small melt pool size and some substrate heating near the melt pool (Figure 6). With successive passes, the laser substrate temperatures remained close to room temperature away from the laser heat source. The axial stress solution shows apparent periodicity that corresponds with the solution time step. Additionally, a jagged pattern near the boundary of activated elements is also evident and correlates with the solution time step size. Due to element inversion in the solid mechanics calculation, residual stress predictions are not available for the 2000 W and 500 W laser models.

The cylindrical button model was run through 22.5 seconds of LENS build time. With progressively increasing build time, shear stress magnitudes and distributions propagated with deposition, but showed similar magnitudes and distributions throughout the build time (Figure 7). Normal stresses showed slightly more evolution in magnitude and distribution compared to shear stresses with deposition (Figure 8). Both shear and normal stresses were on the order of 1.0e+08 Pa and similar magnitudes of stress were also present in the substrate. For the cylindrical build model, displacements were present in both the deposited part as well as the substrate (Figure 9). Maximum displacements were found in the center of the build where initial deposition occurred. Displacement magnitudes increased slightly with increasing build time.

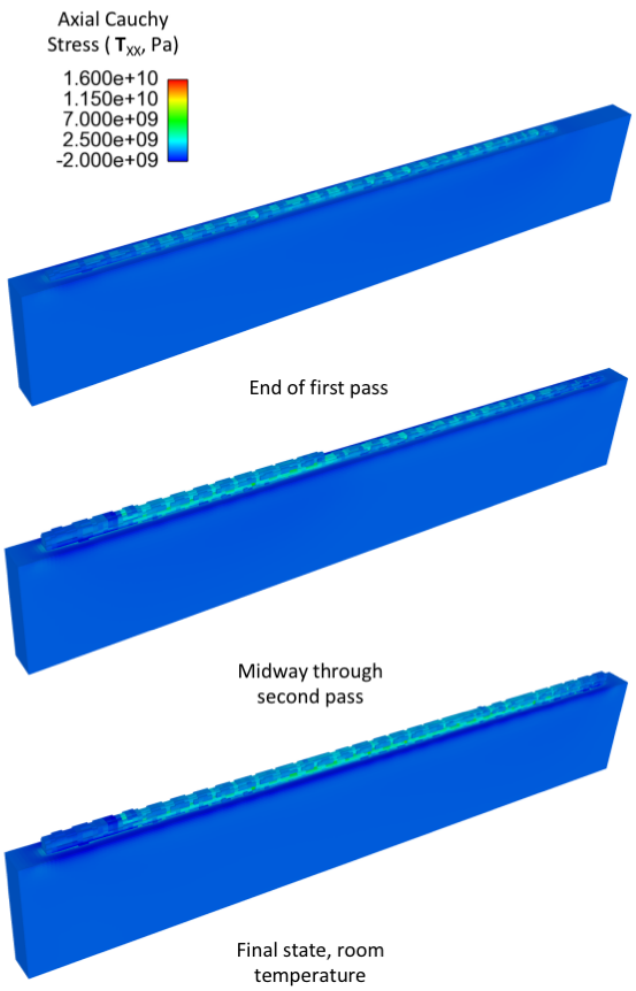

FIGURE 5. AXIAL STRESS ALONG THE LONG AXIS DURING THE FIRST PASS, MIDWAY THROUGH THE SECOND PASS, AND AFTER COOLING FOR VARIABLE LASER POWER THIN WALLED BUILD. CORRESPONDING TEMPERATURE PROFILES ARE SHOWN FIGURE 6.

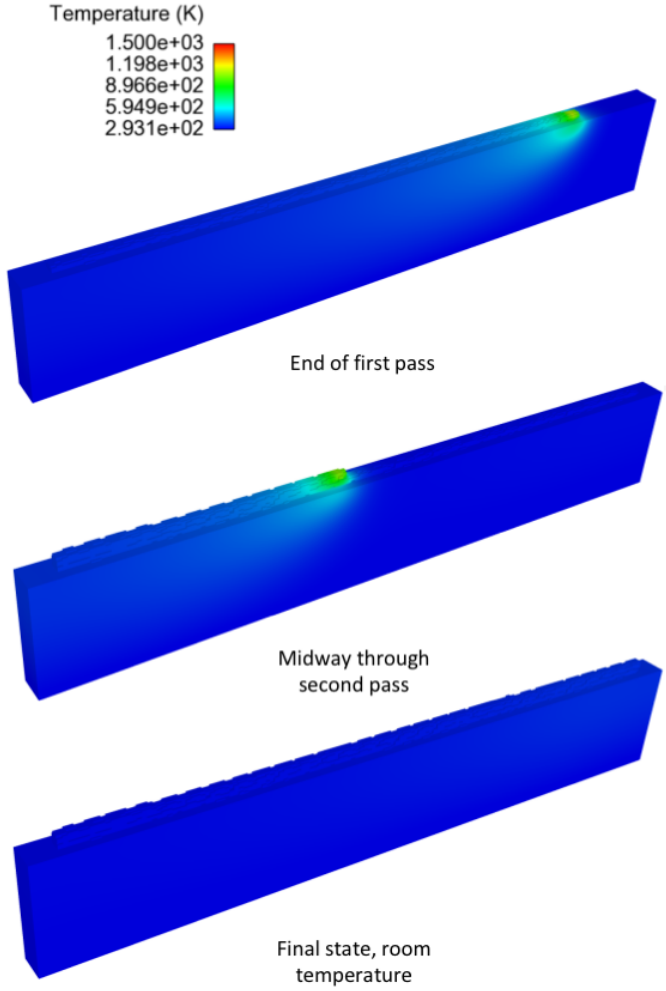

FIGURE 6. TEMPERATURE PROFILES DURING THE FIRST PASS, MIDWAY THROUGH THE SECOND PASS, AND AFTER COOLING FOR THE VARIABLE LASER POWER THIN WALLED BUILD. CORRESPONDING AXIAL STRESSES ARE SHOWN IN FIGURE 5.

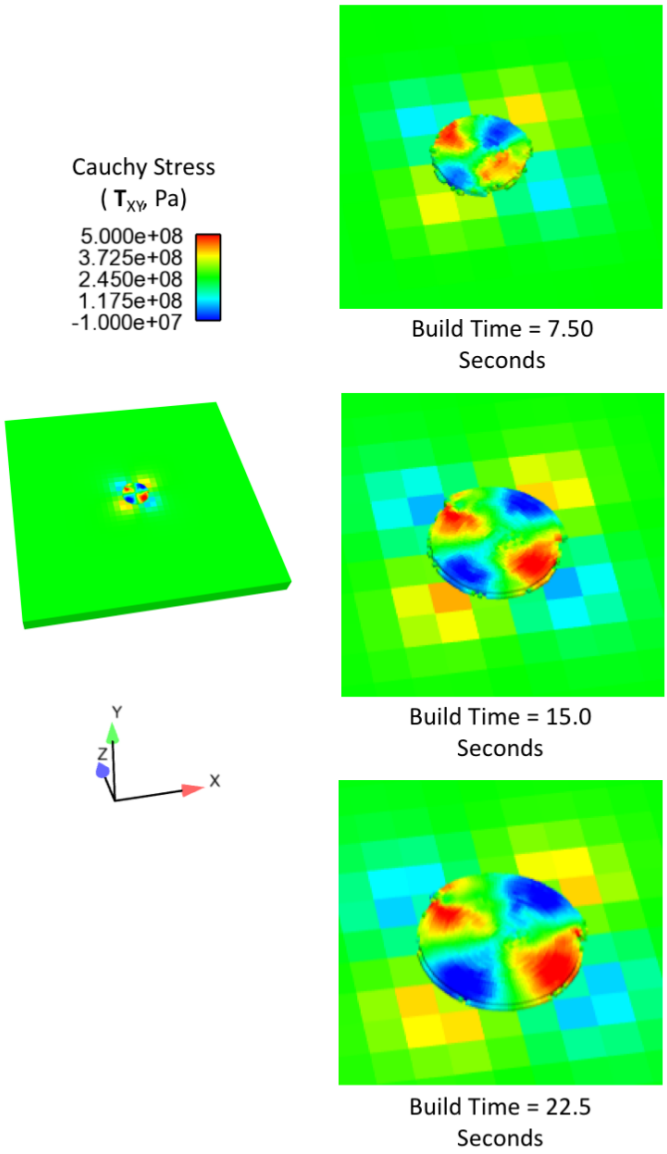

FIGURE 7. SHEAR STRESS IN THE CYLINDRICAL BUTTON LENS BUILD AT VARIOUS BUILD TIMES. CORRESPONDING NORMAL STRESSES ARE SHOWN IN FIGURE 8.

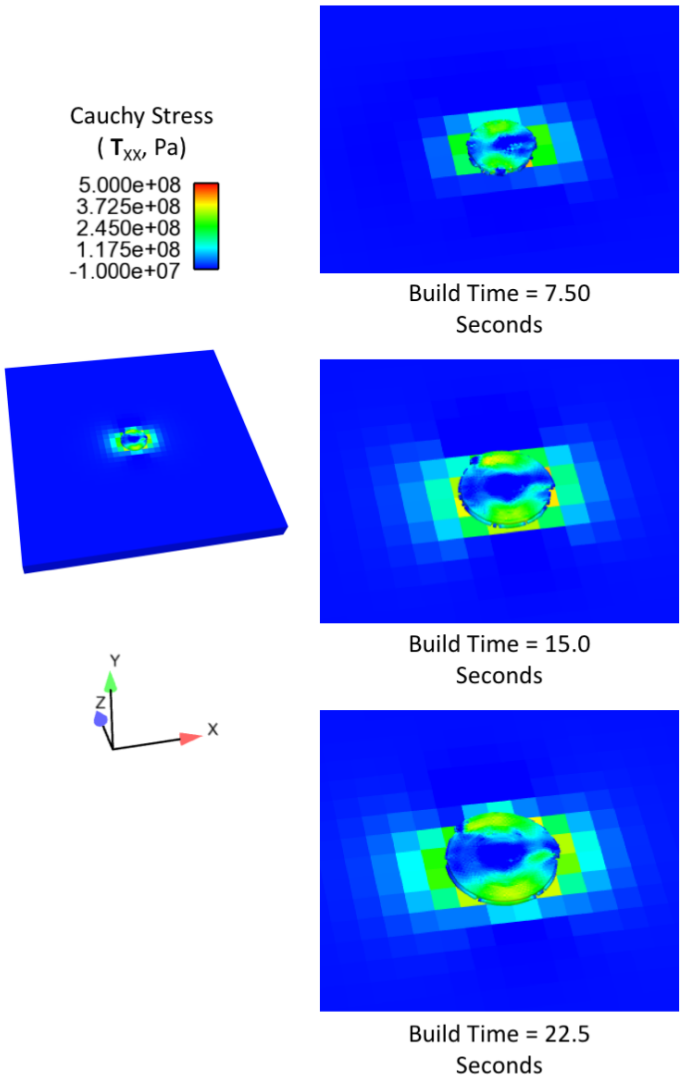

FIGURE 8. NORMAL STRESSES IN THE CYLINDRICAL BUTTON BUILD AT VARIOUS BUILD TIMES. CORRESPONDING SHEAR STRESSES ARE SHOWN IN FIGURE 7.

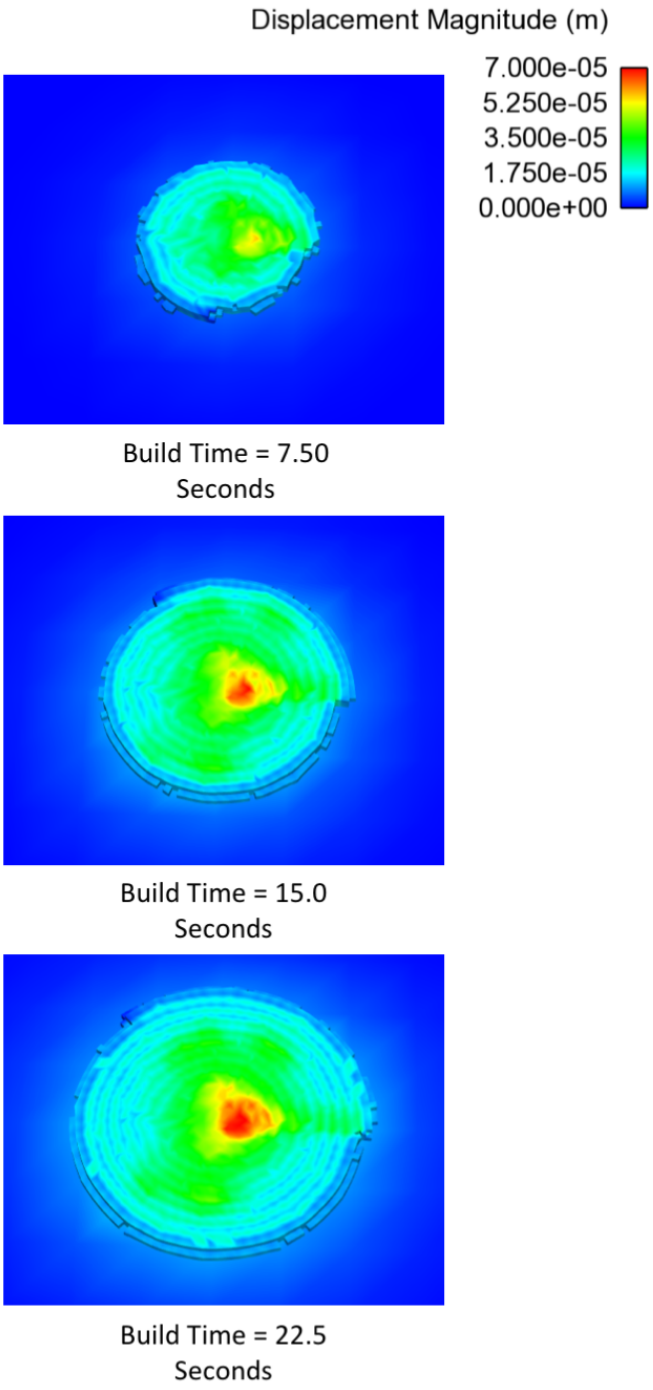

FIGURE 9. DISPLACEMENT MAGNITUDES IN BUTTON PART AFTER 22.5 SECONDS OF LENS BUILD TIME.

DISCUSSION

The proposed finite element methodology for simulating the LENS process captures the deposition and solidification of material in a thermal-mechanical finite element context. Initial results for 304 L stainless steel demonstrate some of the effects of controllable LENS parameters and may allow for process improvement without costly and time consuming experimental analysis. Predictions of thermal profiles and stresses preceding and following the build area are made for thin wall and solid cylinder geometries. Element activation is enabled *via* a spherical laser heat source that activates elements that are determined to reach temperatures above the defined material melt temperature. Activation and thermal profiles are shown to be dependent on laser power and beam diameter. The evolution of stress, temperature, displacements, and material state variables is tracked and passed between thermal solutions, mechanical solutions, and time steps. Through this method, material state variables and evolutions in stress and temperature can be explored throughout the simulation time. Solid and fluid phases are distinguished in this method using differential material models and contact algorithms. Liquid material behavior is defined in elements above material melt temperature using a Newtonian fluid material model, and a frictional sliding contact algorithm. Solid material behavior is defined for elements below material melt temperature with an elastic-plastic material model, and using a tied contact algorithm. Liquid and solid phases are allowed in both the substrate and the deposition blocks. This methodology enables the simulation of the LENS process based on controllable real world LENS process parameters such as laser power, substrate preheat, and laser raster path. These results will help to improve and better understand LENS production with the aim of producing parts with minimized residual stresses, ideal microstructures, and acceptable geometric dimensions.

The initial results presented herein demonstrate the effects of some LENS process parameters on the general magnitudes and distributions of residual stresses, displacements, and temperatures for LENS builds. For example, higher laser power results in a larger volume of deposited material and higher substrate and deposited material temperatures, a result also observed in experiments (14). Furthermore, the magnitudes of residual stresses are within reason when compared to experimental residual stress measurements for powder bed additive manufacturing (23, 24). However, additional experimental measurements of temperature profiles during LENS builds, as well as post-build residual stress measurements would strengthen, and may validate or improve these modeling results.

Several obstacles to quick and full confidence LENS simulation remain, and must be addressed in parallel with experimental validation prior to accurate LENS process simulation. Time step size was shown to affect the residual stress solution as well as the deposited part shape for a thin walled build through as evidenced by periodicity in the stress and deposition

solutions (Figure 5, 6). Additionally, there exists an inherent mesh dependence in the activation scheme where in sub element sized features are not captured. Large elements are less likely to invert, but do not adequately capture high temperature and stress gradients, and geometric features that are smaller than the element size. Additional work is underway to better understand and quantify the effects of mesh resolution in both the deposition block and the substrate. Remeshing and/or adaptive meshing may also be of interest as the highest temperature, and stress gradients are very near to the focal point of the laser. Significant computational resources are required for these simulations which may present an obstacle when simulating larger LENS builds with the same fidelity. Currently, laser pressure, the momentum of incoming powder, and the effects of any gas swirling associated with the powder stream are neglected. In the future, coupling with a computational fluid dynamics solution for melt pool size and temperature may better inform this model. However, with additional coupling, and more complex analyses, computational expense increases, and the required computational time becomes a limiting factor in obtaining computational resources. The results presented herein are highly dependent on the material model used. The material models parameters and models used were developed for forging (33, 34, 35) yet, higher temperature regimes and near melt plasticity likely have a large influence on the residual stress result. Additional development and/or verification of the constitutive model regarding higher temperatures and near melt plasticity may improve the accuracy of these results. Furthermore, it is of interest to incorporate additional microstructural parameters such as grain size and shape, inclusions, and other microstructural parameters into these calculations to better understand the mechanical performance of a finished part. With improved constitutive and/or microstructural models, it may be possible to predict and optimize the strength and hardness distributions in LENS parts through modification of controllable process parameters.

Modern manufacturing methods such as the LENS process do not have the legacy of knowledge that has been developed for traditional manufacturing processes such as forging and casting. Additionally, there is a great interest in the promise of LENS manufacturing and other DED process owing to the ability of producing novel and complex geometries quickly and easily. However, there is limited understanding of the effects of LENS processing especially when compared to traditional manufacturing methods. This project hopes to help bridge the knowledge gap between AM and traditional manufacturing methods without requiring extensive testing or the development of a wide empirical knowledge base. Our future work will focus on examining the sensitivity of this FE methodology to various parameters, with the goal of reducing computational time without sacrificing a quality solution. Additionally, microstructural experimental results will be incorporated to include appropriate microstructural parameters. Other experimental results will be used to validate the temperature profiles and residual stress values form this model. This work will help to enable full confidence LENS production and performance predictions through optimization of controllable LENS process parameters.

ACKNOWLEDGEMENTS

Sandia National Laboratories is a multi-mission laboratory managed and operated by Sandia Corporation, a wholly owned subsidiary of Lockheed Martin Corporation, for the U.S. Department of Energy's National Nuclear Security Administration under contract DE-AC04-94AL85000.

REFERENCES

[1] Frazier, William E. "Metal additive manufacturing: a review." *Journal of Materials Engineering and Performance* 23.6 (2014): 1917-1928.

[2] Wong, Kaufui V., and Aldo Hernandez. "A review of additive manufacturing." *ISRN Mechanical Engineering* 2012 (2012).

[3] P. Aggarangsi and J.l. Beuth. Localized preheating approaches for reducing residual stress in additive manufacturing. Proc. SFF Symp., Austin, pages 709–720, 2006.

[4] Gong, Xibing, Ted Anderson, and Kevin Chou. "Review on powder-based electron beam additive manufacturing technology." *ASME/ISCIE 2012 international symposium on flexible automation*. American Society of Mechanical Engineers, 2012.

[5] Keicher, David M., et al. "Using the laser engineered net shaping (LENS) process to produce complex components from a CAD solid model." *Photonics West 1997*. International Society for Optics and Photonics, 1997.

[6] C.J. Atwood, M.L. Griffith, L.D. Harwell, E. Schlienger, M. Ensz, J.E. Smugeresky, T. Romero, D. Greene, and D. Reckaway. Laser Engineered Net Shaping (LENS): A Tool for Direct Fabrication of Metal Parts. Technical report, Sandia National Laboratories, 1998.

[7] M. Eshraghi and S.D. Felicelli. 9 Advances in Additive Manufacturing. *Additive Manufacturing: Innovations, Advances and Applications*, page 253. 2015.

[8] M.L. Griffith, D.M. Keicher, C.L. Atwood, J.A. Romero, J.E. Smugeresky, L.D. Harwell, and D.L. Greene. Free Form Fabrication of Metallic Components Using Laser Engineered Net Shaping (LENS).

Proceedings of the 7th Solid Freeform Fabrication *Symposium*, pages 125–132, 1996.

[9] W. Hofmeister, M.J. Wert, J.E. Smugeresky, M.L. Griffith, and M. Ensz. Investigation of solidification in the Laser Engineered Net Shaping (LENS) Process. *JOM*, 51(7):1–7, 1999.

[10] Weiping, Liu and J.N. DuPont. Fabrication of functionally graded TiC/Ti composites by laser engineered net shaping. *Scripta Materialia*, 48(9):1337–1342, 2003.

[11] Y. Xiong, J.E. Smugeresky, L. Ajdelsztajn, and J.M. Schoenung. Fabrication of WC-Co cermets by laser engineered net shaping. *Materials Science and Engineering A*, 493(1-2):261–266, 2008.

[12] L.E. Murr, E. Martinez, S.M. Gaytan, D.A. Ramirez, B.I. MacHado, P.W. Shindo, J.L. Martinez, F. Medina, J. Wooten, D. Ciscel, U. Ackelid, and R.B. Wicker. Microstructural architecture, microstructures, and mechanical properties for a nickel-base superalloy fabricated by electron beam melting. *Metallurgical and Materials Transactions A: Physical Metallurgy and Materials Science*, 42(11):3491–3508, 2011.

[13] Mudge, Robert P., and Nicholas R. Wald. "Laser engineered net shaping advances additive manufacturing and repair." *WELDING JOURNAL-NEW YORK*- 86.1 (2007): 44.

[14] M.L. Griffith, M.E. Schlienger, L.D. Harwell, M.S. Oliver, M.D. Baldwin, M.T. Ensz, M. Essien, J. Brooks, C.V. Robino, J.E. Smugeresky, W. Hofmeister, M.J. Wert, and D.V. Nelson. Understanding thermal behavior in the LENS process. *Materials & Design*, 20(2-3):107–113, 1999.

[15] Rasouli, D., et al. "Effect of cooling rate on the microstructure and mechanical properties of microalloyed forging steel." *Journal of materials processing technology* 206.1 (2008): 92-98.

[16] H. Yin and SD Felicelli. Dendrite growth simulation during solidification in the LENS process. *Acta Materialia*, 58(4):1455–1465, 2010.

[17] Y. J. Lan, D. Z. Li, and Y. Y. Li. Modeling austenite decomposition into ferrite at different cooling rates in low-carbon steel with cellular automaton method. *Acta Materialia*, 52(6):1721–1729, 2004.

[18] Riqing Ye, J E Smugeresky, Baolong Zheng, Yizhang Zhou, and Enrique J. Lavernia. Numerical modeling of the thermal behavior during the LENS process. *Materials Science and Engineering: A*, 428(1-2):47–53, jul 2006.

[19] I.a. Roberts, C.J. Wang, R. Esterlein, M. Stanford, and D.J. Mynors. A three-dimensional finite element analysis of the temperature field during laser melting of metal powders in additive layer manufacturing. *International Journal of Machine Tools and Manufacture*, 49(12- 13):916–923, oct 2009.

[20] L. Wang, S. Felicelli, Y. Gooroochurn, P.T. Wang, and M.F. Horstemeyer. Optimization of the LENS R process for steady molten pool size. *Materials Science and Engineering: A*, 474(1-2):148–156, feb 2008.

[21] P Aggarangsi and Jl Beuth. Localized preheating approaches for reducing residual stress in additive manufacturing. Proc. SFF Symp., Austin, pages 709–720, 2006.

[22] N.E. Hodge, R.M. Ferencz, and J.M. Solberg. Implementation of a thermomechanical model for the simulation of selective laser melting. *Computational Mechanics*, 54(1):33–51, apr 2014.

[23] King, W. E., et al. "Laser powder bed fusion additive manufacturing of metals; physics, computational, and materials challenges." *Applied Physics Reviews* 2.4 (2015): 041304.

[24] King, W., et al. "Overview of modelling and simulation of metal powder bed fusion process at Lawrence Livermore National Laboratory." *Materials Science and Technology* 31.8 (2015): 957-968.

[25] A S. Wu, D W. Brown, M Kumar, GF Gallegos, and W E. King. An Experimental Investigation into Additive Manufacturing-Induced Residual Stresses in 316L Stainless Steel. *Metallurgical and Materials Transactions A*, 45(13):6260–6270, sep 2014.

[26] Dongming Hu and Radovan Kovacevic. Sensing, modeling and control for laser-based additive manufacturing. *International Journal of Machine Tools and Manufacture*, 43(1):51–60, 2003.

[27] Kulkarni, K.M. "Review of forging, stamping, and other solid-phase forming processes." *Polymer Engineering & Science* 19.7 (1979): 474-481.

[28] Liu, H. T., et al. "Characterization of the solidification structure and texture development of ferritic stainless

steel produced by twin-roll strip casting." *Materials characterization* 60.1 (2009): 79-82.

[29] Ghosh, Swati and Vivekanand Kain. "Microstructural changes in AISI 304L stainless steel due to surface machining: Effect on its susceptibility to chloride stress corrosion cracking." *Journal of nuclear materials* 403.1 (2010): 62-67.

[30] Ma, Li, et al. "Using design of experiments in finite element modeling to identify critical variables for laser powder bed fusion." *International Solid Freeform Fabrication Symposium*. Laboratory for Freeform Fabrication and the University of Texas Austin, TX, USA, 2015.

[31] Patrick K Notz, Samuel R Subia, Matthew M Hopkins, Harry K Moffat, and R David. Aria 1.5: User Manual SAND2007-2734. Technical report, Sandia National Laboratories, Albuquerque, NM, 2007.

[32] SIERRA Solid Mechanics Team. Sierra/Solid Mechanics 4.40 User's Guide SAND2016- 2707. Technical report, Sandia National Laboratories, 2016.

[33] A.A. Brown and D.J. Bammann. Validation of a model for static and dynamic recrystallization in metals. *International Journal of Plasticity*, 32-33:17–35, may 2012.

[34] A.A. Brown, L.A. Deibler, L.L. Beghini, T.D. Kostka, and B.R. Antoun. Process modeling and experiments for forging and welding. In *SEM*, 2015.

[35] A.A. Brown, T.D. Kostka, B.R. Antoun, M.L. Chiesa, D.J. Bammann, S.A. Pitts, S.B. Margolis, D. O'Connor, and N.Y.C. Yang. Validation of Thermal-Mechanical Modeling of Stainless Steel Forgings. In *XI International Conference on Computational Plasticity Fundamentals and Applications*, 2011.